

CFD modelling of the thermo- and hydro-dynamic capabilities of long-necked plesiosaurs (reptilia, sauropterygia)

Marx, Miguel; Szász, Robert-Zoltán; Lindgren, Johan

Published in:

Proceedings of the Conference on Modelling Fluid Flow

2025

Link to publication

Citation for published version (APA):

Marx, M., Szász, R.-Z., & Lindgren, J. (2025). CFD modelling of the thermo- and hydro-dynamic capabilities of long-necked plesiosaurs (reptilia, sauropterygia). In J. Vad (Ed.), Proceedings of the Conference on Modelling Fluid Flow: CMFF'25 (pp. 238–245). Article CMFF25-037 Budapest University of Technology and Economics.

Total number of authors:

Creative Commons License: Unspecified

General rights

Unless other specific re-use rights are stated the following general rights apply: Copyright and moral rights for the publications made accessible in the public portal are retained by the authors and/or other copyright owners and it is a condition of accessing publications that users recognise and abide by the

- legal requirements associated with these rights • Users may download and print one copy of any publication from the public portal for the purpose of private study
- You may not further distribute the material or use it for any profit-making activity or commercial gain
 You may freely distribute the URL identifying the publication in the public portal

Read more about Creative commons licenses: https://creativecommons.org/licenses/

If you believe that this document breaches copyright please contact us providing details, and we will remove access to the work immediately and investigate your claim.

LUND UNIVERSITY

Download date: 25. Oct. 2025





Conference on Modelling Fluid Flow CMFF'25
The 19th event of the International Conference Series
on Fluid Flow Technologies held in Budapest since 1959

Conference Proceedings

Edited by J. Vad

Proceedings of the Conference on Modelling Fluid Flow CMFF'25

Edited by J. Vad

Department of Fluid Mechanics, Budapest University of Technology and Economics 2025 Budapest, Hungary

ISBN 978-615-112-002-6

Published by the Department of Fluid Mechanics, Faculty of Mechanical Engineering, Budapest University of Technology and Economics

Address:
Bertalan Lajos 4-6., H-1111 Budapest, Hungary
www.ara.bme.hu

INFLUENCE OF A SCANNING BOX ON THE SETTLING TIME
OF MULTI-HOLE PRESSURE PROBES
HAZARD PREDICTION MODELS FOR BATTERY MODULE
AND PACKS: FLAMMABILITY, PARTICLE IGNITED VENT GAS
, ARCING WITHOUT AND WITH PARTICLES
MULTI-OBJECTIVE DESIGN OPTIMIZATION OF A VARIABLE-
PITCH AXIAL FLOW FAN BY USING CFD-BASED META-
MODEL
MODELLING OF PARAMETRIC OSCILLATIONS IN FLOATING
BODIES
LAMINAR – TURBULENT TRANSITION IN HELICALLY COILED
REACTORS. AN EXPERIMENTAL STUDY WITH HIGH-SPEED
PIV
REDESIGNED ADJUSTABLE DIAPHRAGM FOR CONTROLLIN-
G AND MITIGATING THE SWIRLING FLOW INSTABILITIES
FROM THE CONICAL DIFFUSER OF HYDRAULIC TURBINES $_$
MOBILE SEPARATION OF COMPLEX OIL-WATER MIXTURES
WITH AN ADAPTED PITOT PUMP
PREDICTIONS OF PARTICLE TRAJECTORY RESPONSE TO
REYNOLDS NUMBER IN TURBULENT CHANNEL FLOWS
USING ARTIFICIAL NEURAL NETWORKS
ENHANCING PREDICTIVE ACCURACY OF TURBULENT
SUBCOOLED FLOW BOILING USING LES
LASER-OPTICAL VALIDATION AND COMPARATIVE
ANALYSIS OF NUMERICAL HEAT TRANSFER MODELS FOR
SINGLE NOZZLE IMPINGEMENT FLOWS
A CFD STUDY ON THE EFFECT OF DEFORMABLE BLADES
ON CENTRIFUGAL PUMP PERFORMANCE

ASSESSMENT OF RANS TURBULENCE MODELLING
APPROACHES FOR POLLUTANT DISPERSION IN
VEGETATED STREET CANYONS USING PERIODIC
BOUNDARY CONDITIONS
THE EFFECT OF BUBBLE PARAMETERS ON THE MIXING IN
A BUBBLE COLUMN WITH COUNTER-CURRENT LIQUID FLOW
MODULATING VORTEX DYNAMICS AROUND CIRCULAR
CYLINDER VIA ASYMMETRIC CROSS-SECTIONAL PROFILE
MORPHING: A COMPARATIVE STUDY OF CYLINDRICAL AND
ELLIPTICAL CONFIGURATIONS
A CFD STUDY ON DEPOSITION EFFICIENCY IN CASE OF
INHALED AEROSOL MEDICATION
INFLUENCE OF CUT-BACK LEADING EDGES ON
EFFICIENCY AND FUNCTIONALITY FOR AN OPTIMIZED
SEMI-OPEN 2-CHANNEL IMPELLER
DYNAMICS AND COLLISION OF NON-SPHERICAL ELLIPSOID
PARTICLES IN TURBULENT CHANNEL FLOW
EXPLORING TRANSIENT INSTATIONARITIES OF
MECHANICAL LOAD IN THE OPERATION OF WASTEWATER
PUMPS
THE EFFECT OF HOUSING RECESS GEOMETRY ON FIBER
ENTRY INTO THE BACK SHROUD CAVITY OF A
WASTEWATER PUMP
DIRECT NUMERICAL SIMULATION OF THE JET ATOMIZATIO-
N PROCESS OF SHEAR THINNING GEL FUEL
MOLECULAR DYNAMICS SIMULATION OF THE RHEOLOGIC-
AL BEHAVIOUR OF GEL FUELS
EFFICIENT RADIAL-AXIAL JET FOR IMPROVING THE FLEXIBI-
LITY IN OPERATION OF HYDRAULIC TURBINES

OPTIMISATION OF INLET GUIDE VANE FOR LARGE AXIAL
FANS BASED ON BIG DATA ANALYSIS
ESTIMATION OF RELATION BETWEEN PRESSURE
DIFFERENCE AND FLOW RATE IN A FRANCIS-TURBINE
SPIRAL CASE USING NUMERICAL COMPUTATION
DEFINITION AND COMPUTATION OF A FLUTTER SAFETY
MARGIN FOR QUADCOPTERS BY CHAINING TOGETHER
MULTIPLE 2-DOF AEROELASTIC MODELS
DEVELOPMENT OF A CYLINDRICAL-BLADE WIND TURBINE
DRIVEN BY A NECKLACE VORTEX
A THROMBOSIS MODEL FOR BLOOD-CONTACTING
MEDICAL DEVICES
STUDY OF THE MIXING PERFORMANCE OF CURVED BLADE
TURBINES IN A SOLID-LIQUID DUAL IMPELLER STIRRED
SYSTEM
MINIMIZING SEDIMENTATION IN ROUND WASTEWATER
PUMPING STATIONS WITH THE ASSISTANCE OF PHYSICAL
MODELS
CFD MODELLING OF THE THERMO- AND HYDRODYNAMIC C-
APABILITIES OF LONG-NECKED PLESIOSAURS (REPTILIA, S-
AUROPTERYGIA)
A 0D-3D MODEL FOR THE ANALYSIS OF THE TRANSIENT
THERMAL BEHAVIORS OF AN ELECTRIC POWER TRAIN
EQUILIBRIUM POSITIONS AND DYNAMIC BEHAVIOR OF
THERMAL PROLATE PARTICLES IN SHEAR FLOW:
INFLUENCE OF PARTICLE SIZE
A NOVEL SPH MODEL FOR THROMBUS FORMATION
GAS ACCUMULATION BEHAVIOR IN DIVERGING CHANNELS
WITH GROOVES AND BARS OF VARYING SIZES

NUMERICAL ANALYSIS OF THE DECELERATED SWIRLING
FLOW REGIMES OBTAINED BY USING A MAGNETORHEOLO-
GICAL CONTROL DEVICE
MODELING OF FACE MASK FLOW AND DROPLET
FILTRATION
THE CFD-BASED DESIGN OF A BYPASS TUNNEL TO
PROVIDE THE CROSS-FLOW USED IN THE CASE OF BLADE
CASCADE AEROELASTIC STUDY
PIPE FLOW ANALOGY IN A PLANAR MASS-SPRING-DAMPER
SYSTEM
INVESTIGATION OF RADIUS RATIO EFFECTS ON VELOCITY
STATISTICS IN ANNULAR PIPE FLOW USING ONE-DIMENSIO-
NAL TURBULENCE
COMBUSTION- AND POLLUTANT-MODELLING OF DIMETHYL
ETHER IN A SWIRL-STABILIZED COLD AIR BURNER
DEVELOPMENT OF A CEREBRAL PERIPHERAL VASCULATU-
RE MODEL FOR QUANTITATIVE ASSESSMENT OF
COLLATERAL BLOOD FLOW USING SPECT AND 4D FLOW
MRI
EFFECTS OF WALL SLIP ON LARGE-SCALE FLOW IN
TURBULENT RAYLEIGH-BÉNARD CONVECTION
NUMERICAL INVESTIGATION ON THE INFLUENCE OF
INTERNAL CAROTID ARTERY GEOMETRY ON WALL SHEAR
STRESS DISTRIBUTION
A CONSISTENT APPROACH TO ATMOSPHERIC BOUNDARY
LAYER SIMULATIONS USING THE K-ω SST MODEL
LES AND DES OF FLOW AND ICE ACCRETION ON WIND
TURBINE BLADES

ODTLES: LARGE-EDDY SIMULATION WITH AUTONOMOUS	
STOCHASTIC SUBGRID-SCALE MODELING APPLIED TO	
TURBULENT DUCT FLOW	358
NUMERICAL ANALYSIS OF SWIRLING FLOW INDUCED BY	
AXIAL FAN	366
FLOW DIVERTER TREATMENT FOR INTRACRANIAL MEDIA B-	
IFURCATION ANEURYSMS: CHALLENGING THE PREDICTIVE	
ROLE OF MORPHOLOGY AND HEMODYNAMICS	374
NUMERICAL INVESTIGATION OF A LIFTED METHANE/AIR	
JET FLAME USING STOCHASTIC MAP-BASED TURBULENCE	
MODELING	382
NUMERICAL INVESTIGATION OF LIQUID EMBOLIZATION	
FOR INTRAVASCULAR TREATMENT USING A PARTICLE	
METHOD	390
DEVELOPMENT OF THE TURBULENT SWIRLING FLOW	
VELOCITY PROFILES IN THE AXIAL FAN JET	397
EVALUATING THE PROBABILITY OF INFECTION IN A UK	
HOSPICE THROUGH A CFD DRIVEN METRIC	403
NUMERICAL MODEL DEVELOPMENT AND ANALYSIS OF A	
DROP-ON-DEMAND INKJET APPLICATION	412
A NOVEL EULERIAN-LAGRANGIAN MULTI-SCALE METHOD	
FOR CAVITATING FLOW IN AN INJECTOR NOZZLE	421
LOW-AMPLITUDE ACOUSTIC MODULATION AS A TOOL FOR	
CONTROLLING THE VORTEX STRUCTURES OF THE	
TURBULENT AXISYMMETRIC AIR JET	428
BEM SIMULATION OF AN EXPANDING / CONTRACTING	
BUBBLE IN VISCOELASTIC FLUIDS	439
A COMPREHENSIVE ANALYSIS OF VARIABLE INLET GUIDE	
VANE ON CAVITATION AND HYDRAULIC PERFORMANCE OF	
AN AXIAI -FI OW PUMP	446

SPHERICAL STABILITY AND BREAKUP LIMIT OF OSCILLATIN
G MICROBUBBLES
FLUID MECHANICS OF CEREBRAL THROMBI
MODELLING THE TRANSPORT OF OXYGEN IN THE HUMAN
VASCULAR SYSTEM
MODELLING THE METABOLIC AND MYOGENIC CONTROL IN
HUMAN BLOOD CIRCULATION
MULTIPHASE MODEL OF THE MELT BLOWING PROCESS IN
MULTI-HOLE NOZZLES
CAVITATION BUBBLE NEAR A WALL: SENSITIVITY TO
MODELING CONDITIONS
SUPERPOSITION OF SECONDARY FLOWS INSIDE
ARTIFICIAL GEOMETRIES
GEOMETRICAL OPTIMIZATION OF RECTANGULAR MVGS
DELAYING BOUNDARY LAYER TRANSITION OVER A FLAT
PLATE
DESIGN AND DEVELOPMENT OF AN AUTOMATIC PUMP
TEST RIG FOR CONDITION MONITORING OF MECHANICAL
SEALS
SIMULATION AND CHALLENGES FOR A LOW SPECIFIC
SPEED PELTON TURBINE
APPLICATION RANGES OF THE HAGEN-POISEUILLE LAW
TO MODEL NON-NEWTONIAN FLUID-FILLED DAMPERS
EVALUATION OF CAROTID PLAQUE MORPHOMETRY AND H
EMODYNAMICS
IMPACT OF WAVE DIRECTIONALITY AND INTER-DEVICE
SPACING ON THE PERFORMANCE OF WAVE ENERGY
CONVERTER ARRAYS

EXPERIMENTAL AND NUMERICAL INVESTIGATIONS OF	
NOZZLE SPACING EFFECTS ON FLOW CHARACTERISTICS	
OF TRIPLE RECTANGULAR FREE JETS	557
AN APPLICATION OF MACHINE LEARNING TO COMPUTE TH-	
ERMOCHEMISTRY OF REACTIVE FLOWS: A MIXTURE OF	
EXPERTS APPROACH	565
COMBINING THE PARTIALLY STIRRED REACTOR WITH A	
DEM DESCRIPTION: THE PYROLYSIS OF BIOMASS	573
USING JACOBI METHOD TO SOLVE THE TWO-EQUATION	
TURBULENCE MODEL FOR PARALLELIZATION ON GPU	
COMPUTING SYSTEM	_ 581
EXPERIMENTAL AND NUMERICAL INVESTIGATION OF THE	
TURBULENT SWIRLING FLOW IN PIPE BEHIND THE AXIAL	
FAN IMPELLER	588
A NEW VISCOSITY FORMULATION FOR IMPROVED	
TURBULENCE MODELING IN KOLMOGOROV FLOW	595
INVESTIGATION OF LAMINAR STEADY AND UNSTEADY	
FLOWS IN GYROID TPMS STRUCTURES	603
DETAILED CHARACTERISATION OF PORE STRUCTURE AND	
TRANSPORT PROPERTIES OF BIOMASS PARTICLES	
DURING PYROLYSIS	609
INVESTIGATING THE INFLUENCE OF PARTICLE SHAPE ON	
THE PYROLYSIS OF THERMALLY THICK PARTICLES IN DEM	
/CFD	617
NUMERICAL AND EXPERIMENTAL INVESTIGATION OF LOW	
REYNOLDS NUMBER FLOW IN A PACKED BED OF ROTATED	
BARS	625
ENHANCING DEM-CFD SIMULATIONS WITH MACHINE-	
LEARNING-BASED LOCALLY RESOLVED NUSSELT NUMBER	
CORRELATIONS	633

AN OPEN WORKFLOW FOR UNSUPERVISED CLUSTERING	
OF FLUID-PARTICLE FLOWS INTO COMPARTMENTS	64
A COMPRESSIBLE TWO-FLUID MODEL FOR THE	
SIMULATION OF TRIBOELECTRIFICATION	648
INFLUENCE OF PACKING DENSITY ON THE CALCINATION	
PROCESS FOR LIME PRODUCTION: A DEM-CFD STUDY	65
MULTISCALE COMPUTATIONS OF REACTIVE MULTIPHASE	
FLOWS	66
OPTICAL THERMOMETRY COUPLED TO THE MEASUREMEN-	
T OF OTHER QUANTITIES (VELOCITY, PRESSURE)	67
MACROSCOPIC AND MICROSCOPIC BLOOD FLOWS	68
A LOOK BACK ON 30 YEARS OF TURBOMACHINERY	
RESEARCH IN EUROPE	69
Sponsors and Partners	71



CFD modelling of the thermo- and hydrodynamic capabilities of long-necked plesiosaurs (Reptilia, Sauropterygia)

Miguel MARX², Róbert-Zoltán SZÁSZ¹, Johan LINDGREN³

- ¹ Corresponding Author. Department of Energy Sciences, Lund University. PO.Box 118, S-22100, Lund, Sweden. Tel.: +46 46 222 0480, E-mail: robert-zoltan.szasz@energy.lth.se
- ² Department of Geology, Lund University. E-mail: miguel.marx@geol.lu.se
- Department of Geology, Lund University. E-mail: johan.lindgren@geol.lu.se

ABSTRACT

Plesiosaurs are secondarily aquatic reptiles with a fossil record that extends for over 140 million years, and their remains have been found in localities representing both warm, equatorial waters and cold, high-latitude environments. They are usually portrayed as a snake threaded through the body of a sea turtle. However, due to a general absence of preserved soft tissues, reconstructing the life appearance of particularly long-necked forms is anything but a straightforward task. Moreover, animals with such an oddly-shaped body are unlikely to survive in coldwater environments. To investigate the ability of these ancient marine reptiles to inhabit high-latitude waters, we examined the heat transfer in two virtually reconstructed plesiosaurs: one built according to conventional wisdom (i.e., with a long and narrow neck) and one equipped with a peripheral layer of insulating blubber. We compared several modelling approaches (gradually increasing the complexity of our approach) to assess their pros and cons. We also investigated the temperature distribution within the two body types and tested their hydrodynamic performance by simulating a cruising plesiosaur at a steady velocity. The results of our endeavours show that an insulating blubber layer must have been present to assure a suitable temperature distribution within the plesiosaur body when it inhabited cold water re-

Keywords: blubber, heat transfer, plesiosaurs, temperature distribution

NOMENCLATURE

c_p	[J/(kg K)]	specific heat at constant pres-
L	[m]	sure length
MR	[W/kg]	metabolic rate
R	[<i>m</i>]	radius
T	[<i>K</i>]	temperature

t	[<i>s</i>]	time
q	$[W/m^3]$	heat source
α	$[m^2/s]$	thermal diffusivity
K	[W/(m K)]	heat conductivity
ϕ	$[W/m^2]$	heat flux per unit area
ρ	$[kg/m^3]$	density

1. INTRODUCTION

Palaeontology is an interdisciplinary science that incorporates methods from various fields, including Computational Fluid Dynamics (CFD) [1]. Plesiosaurs (an iconic group of Mesozoic marine reptiles) have garnered some attention in recent years due to their peculiar body shape (long neck, turtlelike body, and four flippers), making them interesting subjects for CFD analyses [2, 3]. While some experiments have been conducted on their swimming performance [2, 3], little is known about their thermodynamic capabilities. Notably though, plesiosaur fossils have been recovered from high-latitude environments [4, 5], to suggest that they were capable of surviving in cold water regimes, something that likely would have necessitated some sort of insulation. Modern whales and even a species of sea turtle (Dermochelys coriacea; the Leatherback turtle) utilize a combination of high metabolism, large body size and blubber (a peripheral insulating tissue) to resist the effects of cold water. Blubber was apparently also present in at least some derived ichthyosaurs, another group of extinct marine reptiles [6]. Thus, we hypothesize that plesiosaurs, in which endothermy (warm-bloodedness) has been proposed [7, 8, 9], likewise employed some sort of peripheral tissue layer to enable life in cold water environments.

Modelling heat transfer in an animal poses a number of challenges. To start with, there are several body regions (e.g., muscles, the brain) with heat production that are hard to assess. The heat conductivity of tissues is also difficult to measure accurately, and the circulatory system that regulates heat transfer

between different body parts is challenging to model [10]. Furthermore, if a species is extinct, then the required parameters have to be estimated from analogies in living animals.

Several models are available that replicate physical phenomena involved in heat transferring processes. However, by adding more details, the complexity of the models is amplified, in turn increasing both the required computing resources and human efforts to set-up and analyse the cases. Furthermore, when there are several unknown parameters, a model with increased complexity does not necessarily yield better results.

The purpose of this study is to compare modelling approaches at different levels of complexity to simulate a plesiosaur living in a cold water environment. We also test the effects of an added blubber layer on hydrodynamic drag.

2. METHODS

2.1. One-dimensional analysis

The simplest model assumes that the blubber layer thickness is small relative to the surface area of the skin. For such a condition, the heat transfer through the blubber can be presumed to be one-dimensional and thus assessable by Fourier's law of heat conduction (Eq. 1). Fourier's law can be used, e.g., to estimate the heat flux if the heat conductivity, blubber thickness and temperature difference between the surrounding environment and inner body temperature are known.

$$\phi = -\kappa \frac{\Delta T}{\Delta x} \tag{1}$$

For this initial model, blubber thicknesses and thermal conductivity values for various whale species were adapted from [10, 11] and references therein. Leatherback turtle blubber thickness was obtained from [12], and the thermal conductivity value was assumed to be $0.24 \ W/(m \ K)$. The thermal conductivity value for human fat was acquired from [11].

2.2. Cylindrical model

Due to their overall elongate body form, the heat transfer characteristics of several marine animals were investigated by assuming a cylindrical shape. For example, Hokkanen [10] studied the temperature regulation of marine mammals using such a model. By neglecting end-effects, heat transfer can be evaluated in one (radial) direction. This model has the advantage of considering volume and surface area effects compared to the one-dimensional model presented in the previous sub-section.

Here, we estimated the heat flux transferred across a blubber layer with an inner radius R_{in} and outer radius R_{out} for an animal of length L using Eq. 2[13].

$$Q = 2\pi\kappa L \frac{\Delta T}{ln(R_{out}/R_{in})} \tag{2}$$

The heat flux was calculated using body dimensions of the modern Right whale [10, 14], Harbour porpoise [10, 15], Leatherback turtle [12, 16], and two plesiosaur models: one with a thin (1 cm) layer of blubber and a second geometry with a thicker (7 cm) layer of blubber; the required parameters being adopted from [10, 12, 14]. The total length of the plesiosaur cylinder model was set to 11.7 meters based on a reconstruction of the extremely long-necked elasmosaurid, *Albertonectes vanderveldei* (TMP 2007.011.0001).

2.3. 3D heat conduction

Heat conduction in an arbitrary threedimensional geometry, which can include heat sources, can be investigated by solving the Poisson equation (Eq. 3). For this purpose, the laplacian-Foam solver implemented in OpenFOAM v.2306 [17] was used.

$$\frac{\partial T}{\partial t} = \nabla \cdot (\alpha \nabla T) + \frac{q}{\rho c_p} \tag{3}$$

Two plesiosaur geometries were constructed using FreeCAD [18]: one without blubber and a second one coated in an insulating layer (based on actual blubber thicknesses of the Leatherback turtle [12]). The total length of the geometry was set to 11.7 meters. The thickness of the muscle tissues encasing the skeleton was approximated from comparisons with modern reptiles [19, 20, 21]. In the blubbercoated model, this peripheral tissue was added to all parts of the body except the flippers. Figure 1 shows a perspective view of the reconstructed geometry without (top) and with blubber (bottom).

The heat conductivity of blubber ($\approx 0.30~W/(m~K)$) is significantly lower than that of muscles ($\approx 0.57~W/(m~K)$) [10]; therefore, it is important to investigate the impact of regions with different heat conductivity on the resulting thermal balance. Furthermore, the heat source in the present case is due to metabolism, which depends on the activity level of the animal [22].

As a result, a third geometry was created to include simplified viscera (internal organs), arteries and a brain (which, for simplicity, hereafter is referred to as the 'organ region'). This simplified region is located inside the reconstructed plesiosaur body as shown in Figure 2. The division of the geometry into multiple regions primarily affects the mesh generation process. At the interfaces separating the regions, internal boundaries (referred to as 'baffles' in OpenFOAM terminology) are introduced. Additionally, the mesh is refined in these regions to better capture temperature gradients. From the solver's perspective, the entire mesh remains as a single computational domain; the purpose of the

various regions is solely to assign different material properties.

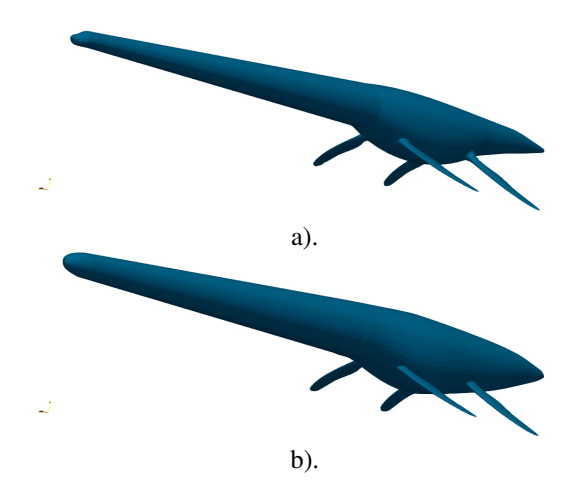


Figure 1. Perspective view of the adopted plesiosaur geometry a) without and b) with blubber.



Figure 2. Side view of the adopted plesiosaur geometry with the internal region marked in red.

Tissues in the geometries were assigned thermal conductivity values reported for extant marine animals: muscle and organ region $(0.57 \ W/(m \ K))$ [10], and blubber $(0.30 \ W/(m \ K)) \ [10, 11, 22]$. In certain cases, the thermal conductivity of the blubber was adjusted to $0.57 \ W/(m \ K)$ to replicate vasodilation of the circulatory system in the blubber tissue [23], since this is a known physiological adaptation of marine animals [10, 24]. A specific heat of $3.75 \ kJ/(kg \ K)$ was applied to all tissues [22]. Two different metabolic rates were assigned to the models: a lower rate ($MR = 0.083 \ W/kg$) corresponding to an inactive cold blooded animal, and an elevated value (MR = 1.51 W/kg) typical of a Leatherback turtle exercising [24]. The heat-generating regions were either assigned to the entire body or only to the organ region. A metabolic rate was not, however, assigned to the blubber as this is not a heat generating tissue. A water temperature of $12^{\circ}C$ (285.15 K) was chosen because it is comparable to what A. vanderveldei would have experienced [4]. Prescribing the water temperature directly on the skin neglects the thermal boundary layer formed in the water in the immediate vicinity of the body. As a consequence, the cooling effect of the water is over predicted. Nevertheless, according to the analysis in [10], the associated error likely is small.

2.4. Hydrodynamic force computations

In addition to heat balance, an added blubber layer affects the hydrodynamic forces acting on the body. In order to estimate this impact, two additional computations were performed. The flow around the two plesiosaur geometries was solved using the simpleFoam solver included in OpenFOAM v.2306. The pressure-velocity coupling is based on the SIMPLE algorithm (see, e.g., [25]). The computational domain extended from (-40 m, -25 m, -25 m) to (100 m. 25 m. 25 m) (Figure 3), the model being located at (0,0,0). The k-omega SST turbulence model developed by Menter [26, 27] was employed. The velocity magnitude was set to 1.5 m/s; i.e., close to the estimated cruising speed of other extinct marine reptiles [28]. A sensitivity study involving grids with 1.2, 3.0, 9.1, and 31.4 million cells indicated that 9.1 million cells were sufficient for our purposes.

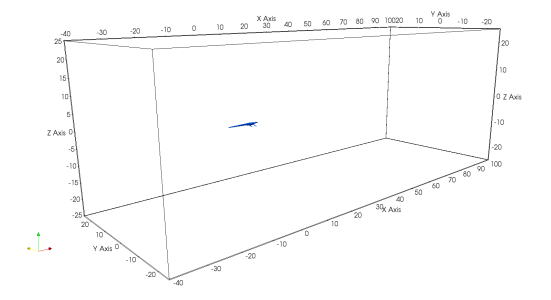


Figure 3. The computational domain used in our flow computations.

3. RESULTS

3.1. One-dimensional analysis

The effects of blubber thickness and the thermal conductivity of this tissue can be clearly seen in Figure 4. The proportionally thin layer of fat in a human allows for a larger heat flux relative to fluxes predicted for cetaceans that have both thicker blubber and lower thermal conductivity values. Notably, a plesiosaur inhabiting cold water environments would benefit from possessing a peripheral layer of insulating blubber.

3.2. Cylindrical model

Using Eq. 2, the total heat flux was estimated for two versions of the modelled plesiosaur (one with and one without blubber), as well as for a number of comparative extant tetrapods. The adopted parameters and the estimated heat fluxes for an assumed temperature difference of $\Delta T = 20 \, K$ are summarized in Table 1.

A Northern right whale (a species that is well-adapted for life in cold waters) at approximately the same length as our modelled plesiosaur (~12 meters), but with a greater volume and blubber thickness, has a significantly lower heat flux compared to the plesiosaur version without blubber. An addition of seven

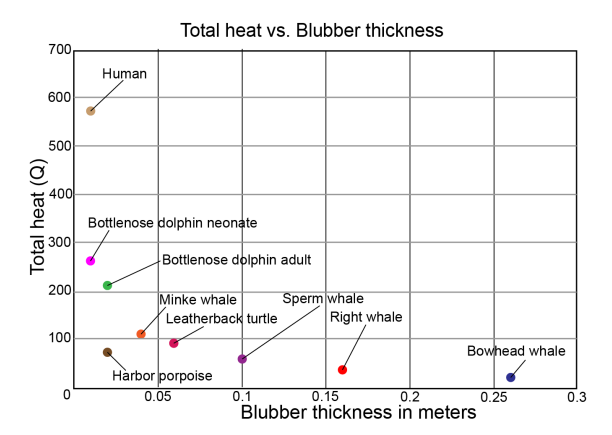


Figure 4. Predicted heat flux values for select extant tetrapods.

Table 1. Heat flux predicted for plesiosaurs and select modern animals.

Animal	Rout	R_{in}	L	κ	Q
	[<i>m</i>]	[<i>m</i>]	[m]	$\left[\frac{W}{mK}\right]$	[W]
Harbour por- poise	0.08	0.06	1.6	0.1	70
Right whale	1.45	1.29	12	0.3	3867
Leatherback Turtle	0.52	0.45	2	0.3	1093
Plesiosaur (no blubber)	0.43	0.42	11.7	0.3	18736
Plesiosaur (blubber)	0.49	0.42	11.7	0.3	2860

centimetres of blubber (which is similar to the blubber layer covering an adult Leatherback turtle) to the plesiosaur model significantly reduces the heat flux to an order of magnitude that is comparable to that of the other considered species. This reduction suggests that plesiosaurs would have benefited from an insulating blubber layer.

3.3. Three-dimensional heat transfer calculations

The purpose of these computations was to investigate the temperature within the plesiosaur body in a variety of scenarios. In all simulations, the water temperature was set to $12^{\circ}C$. Moreover, based on experiments conducted on hatchling sea turtles [29], the lowest temperature that a plesiosaur probably could comfortably tolerate is $15^{\circ}C$, whereas the highest temperature is $40^{\circ}C$. Hence, the color scales used in the figures that follow span the 12– $40^{\circ}C$ interval (i.e., 285.15–313.15 K) (Optimal temperatures are considered to be regions coloured either darkblue or red).

There are two important regions to consider. Firstly, due to the long and narrow neck, the water might cool the brain to dangerously low temperatures. Secondly, the torso has a low surface area-to-volume ratio, and thereby may be prone to overheat-

ing.

We investigated the impact of the main parameters (such as the metabolic rate, heat conductivity and presence of a peripheral blubber layer) on the temperature distribution in the body. Additionally, a case with three regions was set-up, where the effect(s) of enhanced heat transfer due to an introduced circulatory system was modelled, albeit in a simplified manner.

3.3.1. Influence of metabolic rate

The impact of metabolic rate on the temperature distribution was evaluated for a model without blubber. Two extreme cases were considered: one corresponding to an inactive individual ($MR = 0.083 \ W/kg$) and one to a highly active animal ($MR = 1.585 \ W/kg$). In both cases, the heat conductivity was set to $0.57 \ W/(m \ K)$.

In the low activity case (Fig. 5), the temperatures across the body are suboptimal, the head and neck essentially being of the same temperature as the surrounding water. It is exceedingly unlikely that a plesiosaur would have survived under such conditions over an extended period of time. Conversely, in the high-activity case, the temperatures are closer to optimal in the brain region; however, in the torso they are too high for comfort.

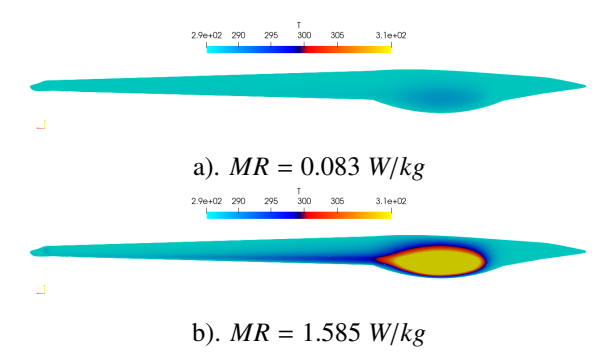


Figure 5. Temperature distribution in a plesiosaur model without blubber at low a) and high b) metabolic rates, respectively ($\kappa = 0.57 \ W/(m \ K)$).

3.3.2. Influence of heat conductivity

The heat conductivity can vary not only between tissues, but also for the same tissue depending, e.g., on the influence of the circulatory system. Three values were considered. The lowest one ($\kappa = 0.30 \, W/(m \, K)$) is typical for blubber [10], whereas the second one ($\kappa = 0.57 \, W/(m \, K)$) is representative of muscles. The third considered value ($\kappa = 2.0 \, W/(m \, K)$) was adopted to mimic improved heat transfer by convection effects caused by the circulatory system.

Figure 6 shows the temperature distribution for the low metabolic rate case. As expected, higher heat conductivity values lead to a more uniform heat distribution, but also to a stronger cooling effect in the torso region.

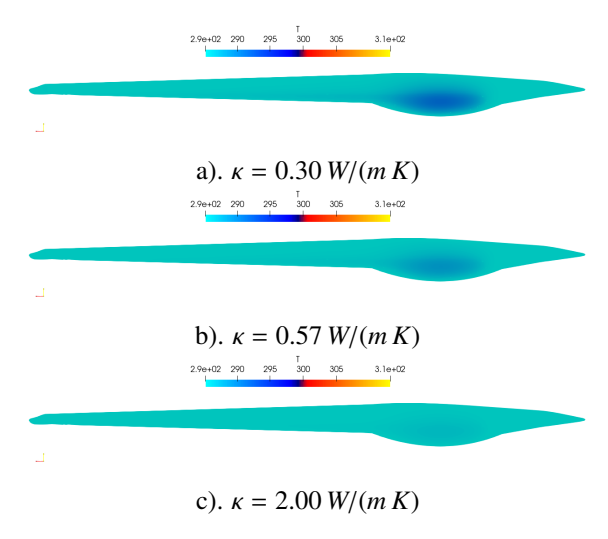


Figure 6. The impact of heat conductivity on the temperature distribution in the plesiosaur without blubber. $MR = 0.083 \ W/kg$

3.3.3. Influence of blubber

The temperature distribution of a plesiosaur model covered by an external blubber layer was evaluated for a number of metabolic rates and heat conductivity values. In Figure 7, three parameter combinations are depicted.

Figure 7a shows the temperature distribution in a low metabolic rate case. Here, the heat conductivities are typical of muscle and blubber tissues. Compared to the corresponding setup of the case without blubber (Fig. 6a), it is noticeable that there are more favourable temperatures in most parts of the body. Nevertheless, in the brain region, the predicted temperatures are still very low.

In the second case (Fig. 7b), the blubber heat conductivity is increased to $0.57 \, W/(m \, K)$. Such a condition could mimic, e.g., improved heat transfer due to vessel dilatation. As expected, there is a stronger cooling effect in the body, but the temperatures are still more viable than in the case without blubber (Fig. 6b).

The third case is characterised by a high metabolic rate (Fig. 7c). Even if the blubber heat conductivity is set to higher values (typical of muscles), and therefore a more intense cooling is assumed, the predicted temperatures for most parts of the body remain too elevated, suggesting that the analysed metabolic rate is too high for the adopted blubber layer thickness.

3.3.4. Three-region model

Heat transfer due to convection by blood is an important phenomenon that is difficult to account for. Due to the range of the involved scales, an explicit computation, even if restricted to the larger diameter parts of the vascular system would still be too demanding from a computational point of view. Accordingly, here we employed a sim-

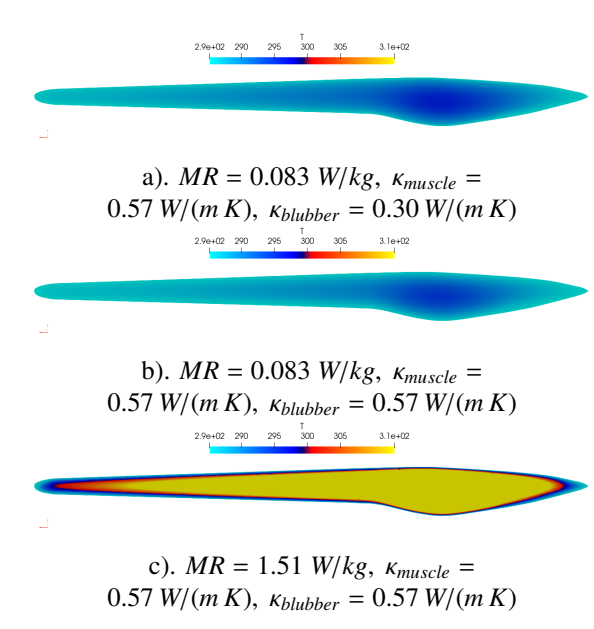


Figure 7. Impact of blubber layer on the temperature distribution.

plified approach where the convective heat transfer by the vascular system is accounted for by an increased heat conductivity coefficient. According to Hokkanen [10], realistic blood flow rates are in the range of 1–4 $kg/(m^3 s)$ which cause a heat transfer of approximately $4000-16000 \ W/(m^3 K)$. By dimensional analysis, the adopted heat conductivity coefficient ($\kappa = 2 \ W/(m \ K)$) results in cross sectional area magnitudes of $125-500 \ mm^2$, which are reasonable, given the size of the animal (the largest diameter of the torso is approximately $1 \ m$).

In the three-region set-up, the outermost region corresponded to blubber ($\kappa = 0.30 \, W/(m \, K)$), the middle region muscle ($\kappa = 0.57 \, W/(m \, K)$) and the inner region was adjusted for higher heat transfer rates ($\kappa = 2 \, W/(m \, K)$). The metabolic rate was set to a high level (MR = 1.51); however, heat was generated only in the core region of the body. The resulting temperature distribution is shown in Figure 8. One may notice the relatively strong heat transfer in the inner region (compare, e.g., with Fig. 5b), which results in more favourable temperatures in the brain region. In the torso, the temperatures remain elevated, to suggests that an added blubber layer likely is unnecessary in this region.

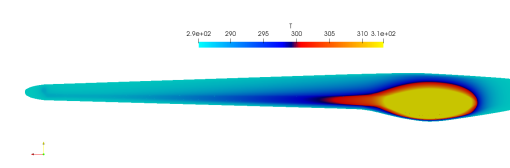


Figure 8. Temperature distribution in the three-region model.

3.3.5. Summary of the three-dimensional cases

quantitative summary of dimensional cases is shown in Figure 9, where the recorded temperatures are plotted at two monitoring points: the first one located near the brain and the second one located close to the centre of the torso. For reference, the inferred minimum and maximum viable temperatures are also plotted. There are several cases where the torso temperature is within viable limits. Conversely, there is only one case where the brain temperature is suitable for survival. However, in that particular case the torso temperature significantly exceeds the upper allowable limit. Nevertheless, there are other cases where the brain temperature is close to the lower limit. With slightly higher metabolic rates than the minimum value and with less insulation in the torso region, both the brain and torso temperatures should be within viable limits.

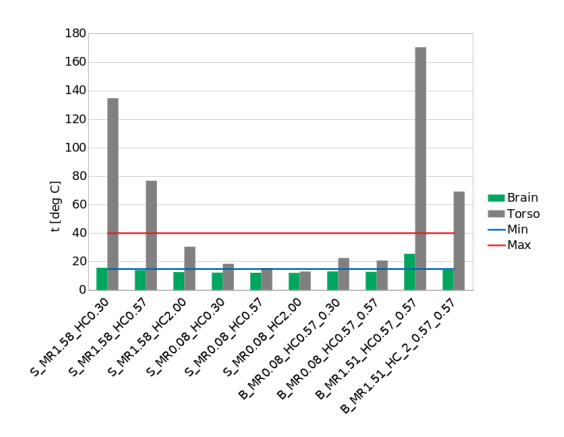


Figure 9. Summary of the observed temperatures in monitoring points located in the brain and torso areas. The labels along the horizontal axis indicate each case. 'S' stands for cases without blubber, 'B' for the ones with an extra blubber layer. The number after 'MR' shows the metabolic rate, while the numbers after 'HC' indicate the heat conductivities.

Models with increased complexity lead to longer computation times. Table 2 summarizes the typical execution times to convergence when running 16 parallel processes on an AMD Ryzen 9 7950X3D 16-core processor. As expected, execution time increases significantly with higher mesh resolution. Moreover, higher thermal conductivity values result in faster convergence, suggesting that longer timesteps could have been used for the lower conductivity cases. Nevertheless, the required computing times are relatively short compared to the more complex CFD simulations, and the impact of suboptimal timestep selection is considered to be negligible.

Table 2. Typical CPU times.

Case type	MR	К	N _{cells}	t_{conv}	
	$\left[\frac{W}{kg}\right]$	$\left[\frac{W}{mK}\right]$	$[.10^6]$	[<i>s</i>]	
No blubber	1.58	0.30	1.9	509	
No blubber	1.58	0.57	1.9	314	
No blubber	1.58	2.00	1.9	134	
No blubber	0.083	0.30	1.9	430	
No blubber	0.083	0.57	1.9	307	
No blubber	0.083	0.30	1.9	137	
With blubber	1.51	0.57	3.8	5260	
with blubber	1.31	0.57			
With blubber	0.83	0.57	3.8	6434	
With blubber	0.65	0.30	3.6	0434	
With blubber	0.83	0.57	3.8	5496	
With blubber	0.63	0.57	3.6		
	1.51	2.0			
Three regions		0.57	16.2	35036	
		0.25			

3.4. Flow computations

These computations were performed to evaluate the impact of the added blubber layer on hydrodynamic drag. Figure 10 shows the pressure distribution along the surface of both the original (top) and blubber-coated (bottom) geometries. No significant difference can be seen in the pressure distributions, which is quantitatively reflected in a tiny (1%) increase of the drag force from 100.92 (original geometry) to $101.93\ N$ (with blubber). This minor rise indicates that the addition of blubber did not lead to any significant penalty in hydrodynamic performance of the selected body shapes.

4. DISCUSSION AND SUMMARY

The impact of an added blubber layer on the heat balance of a plesiosaur (marine reptile) was investigated using numerical models of varying complexity. The simple one-dimensional and cylindrical models predicted a need for an extra insulating layer to reduce the simulated heat fluxes to levels observed in modern animals living in cold-water environments.

The three-dimensional computations further showed that a peripheral insulatory layer was a necessity to achieve a viable internal body temperature. Without an extra blubber layer, the predicted internal temperatures were lethally low for animals at low metabolic rates. Conversely, when a high metabolic rate was introduced, the predicted core temperatures were abnormally high. Nevertheless, as a consequence of the long and slender neck, the temperatures in the brain region remained too low for a real animal.

The addition of a layer of blubber significantly improved the viability chances for individuals with low metabolic rates. For a highly active animal, the added insulation turned out to be too much; the predicted temperature levels exceeded the viable limits in the majority of the body. This suggests that,

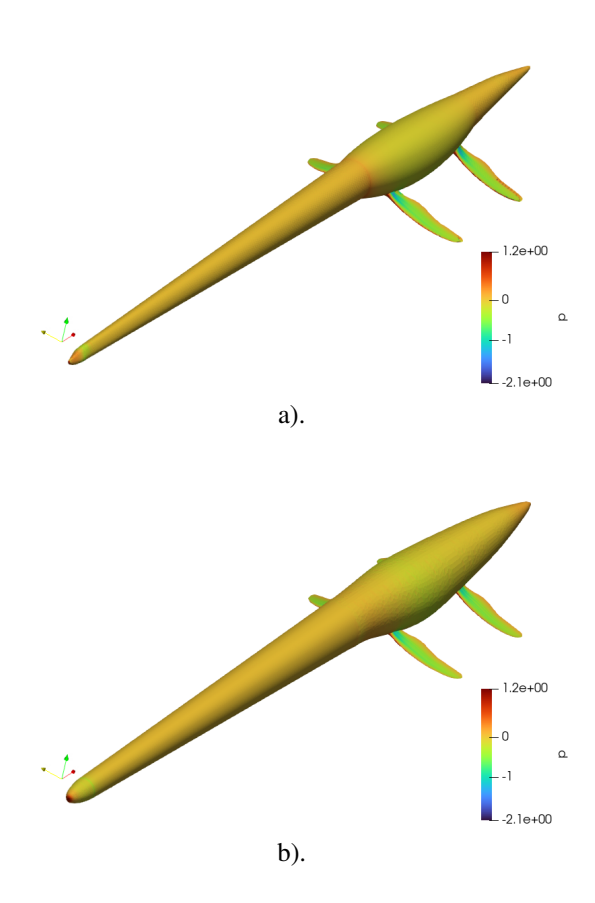


Figure 10. Pressure distribution along the body for a case a) without and b) with blubber

in reality, the thickness of the blubber was probably rather thin in certain regions of the body.

There are several inherent uncertainties in the presented predictions. First of all, there is no widely accepted overall body shape for a plesiosaur; our geometry is a simplification of the general body design, based on a real specimen [30]. The thermodynamic properties of tissues were further approximated based on data from modern animals. Most of these vary between organs and tissues, and sometimes even for the same tissue. Nevertheless, our sensitivity study adopted realistic extreme values. Thus, real-case scenarios are expected to occur within the predicted limits.

The predictions also significantly simplified the heat generation within the body. For better accuracy, several heat generation zones of different magnitudes would be needed. Unfortunately, the information required to set up such simulations is, at present, scarce.

Another limiting factor in the accuracy of our predictions is the difficulty to account for heat convection by the vascular system. A simple model was adopted to account for this phenomenon, but more advanced modelling approaches are expected to substantially improve the accuracy of this parameter.

The adoption of a constant temperature bound-

ary condition implies that the cooling effect of the surrounding water is overpredicted by our models. Although the published literature suggests that this effect is small, it will be verified in the future by a conjugate heat transfer simulation.

We conclude that even if there are unavoidable sources of error in the predictions presented in this paper, our results nonetheless suggest that the currently widely accepted plesiosaur body shape needs to be refined by the addition of a peripheral blubber layer.

ACKNOWLEDGEMENTS

The computations were enabled by resources provided by the National Academic Infrastructure for Supercomputing in Sweden (NAISS), which is partially funded by the Swedish Research Council through grant agreement no. 2022-06725. Additional financial support was provided by a project grant (no. 2020-03542) from the Swedish Research Council awarded to Johan Lindgren.

REFERENCES

- [1] Gutarra, S., and Rahman, I., 2022, "The locomotion of extinct secondarily aquatic tetrapods", *Biological Reviews*, Vol. 97 (1), pp. 67–98.
- [2] Troelsen, P.V.and Wilkinson, D., Seddighi, M., Allanson, D., and Falkingham, P., 2019, "Functional morphology and hydrodynamics of plesiosaur necks: does size matter?", *Journal of Vertebrate Paleontology*, Vol. 39 (2).
- [3] Gutarra, S., Stubbs, T., Moon, B., Palmer, C., and Benton, M., 2022, "Large size in aquatic tetrapods compensates for high drag caused by extreme body proportions", *Communications Biology*, Vol. 5, p. 380.
- [4] Petersen, S., Tabor, C., Lohmann, K., Poulsen, C., Meyer, K., Carpenter, S., Erickson, J., Matsunaga, K., Smith, S., and Sheldon, N., 2016, "Temperature and salinity of the Late Cretaceous Western Interior Seaway", *Geology*, Vol. 44 (11), pp. 903–906.
- [5] Rogov, M. A., Zverkov, N. G., Zakharov, V. A., and Arkhangelsky, M. S., 2019, "Marine reptiles and climates of the Jurassic and Cretaceous of Siberia", *Stratigraphy and Geological Cor*relation, Vol. 27, pp. 398–423.
- [6] Lindgren, J., Sjövall, P., T. V., Zheng, W., Ito, S., Wakamatsu, K., and et al., 2018, "Soft-tissue evidence for homeothermy and crypsis in a Jurassic ichthyosaur", *Nature*, Vol. 564 (7736), pp. 359–365.
- [7] Wiemann, J., Menéndez, I., Crawford, J., Fabbri, M., Gauthier, J., Hull, P., Norell, M., and Briggs, D., 2022, "Fossil biomolecules reveal

- an avian metabolism in the ancestral dinosaur", *Nature*, Vol. 606, pp. 522–526.
- [8] Fleischle, C., Wintrich, T., and Sander, P., 2018, "Quantitative histological models suggest endothermy in plesiosaurs", *PeerJ*, Vol. 6 (e4955).
- [9] Bernard, A., Lécuyer, C., Vincent, P., Amiot, R., Bardet, N., Buffetaut, E., and et al., 2010, "Regulation of body temperature by some Mesozoic marine reptiles", *Science*, Vol. 328 (5984), pp. 1379–1382.
- [10] Hokkanen, J., 1990, "Temperature regulation of marine mammals", *Journal of Theoretical Biology*, Vol. 145, pp. 465–485.
- [11] Dunkin, R. C., McLellan, W. A., Blum, J. E., and Pabst, D. A., 2005, "The ontogenetic changes in the thermal properties of blubber from Atlantic bottlenose dolphin Tursiops truncatus", *Journal of Experimental Biology*, Vol. 208 (8), pp. 1469–1480.
- [12] Wyneken, J., 2015, "Anatomy of the Leatherback Turtle", *The Leatherback Turtle Biology* and Conservation, Johns Hopkins University Press, pp. 34–50.
- [13] Cengel, Y., 2004, *Heat Transfer: A Practical Approach*, McGraw-Hill Education, ISBN 9780071236447.
- [14] Christiansen, F., Dawson, S., Durban, J., Fearnbach, H., Miller, C., Bejder, L., and et al., 2020, "Population comparison of right whale body condition reveals poor state of the North Atlantic right whale", *Marine Ecology Progress Series*, Vol. 640, pp. 1–16.
- [15] Read, A., Keener, W., Webber, M., and Siebert, U., 2025, "Harbour porpoise Phocoena phocoena (Linnaeus, 1758)", *Handbook of Marine Mammals*, Academic Press., p. 427.
- [16] Price, E., Wallace, B., Reina, R., Spotila, J., Paladino, F., Piedra, R., and Velez, E., 2004, "Size, growth, and reproductive output of adult female leatherback turtles Dermochelys coriacea", *Endangered Species Research*, Vol. 1, pp. 41–48.
- [17] OpenFOAM, "OpenFOAM, https://www.openfoam.com", URL https://www.openfoam.com, checked 2025.02.18.
- [18] FreeCAD, "FreeCAD, https://www.freecad.org", URL https://www.freecad.org, checked 2025.02.18.
- [19] Cieri, R., 2018, "The axial anatomy of monitor lizards (Varanidae)", *Journal of Anatomy*, Vol. 233 (5), pp. 636–643.

- [20] Klingler, J., 2016, "On the morphological description of tracheal and esophageal displacement and Its phylogenetic distribution in Avialae", *Plos one*, Vol. 11 (9), p. e0163348.
- [21] Davenport, J., Fraher, J., Fitzgerald, E., McLaughlin, P., Doyle, T., Harman, L., and Cuffe, T., 2009, "Fat head: an analysis of head and neck insulation in the leatherback turtle (Dermochelys coriacea)", *Journal of Experimental Biology*, Vol. 212 (17), pp. 2753–2759.
- [22] Bostrom, B., and Jones, D. R., 2007, "Exercise warms adult leatherback turtles", *Comparative Biochemistry and Physiology Part A: Molecular Integrative Physiology*, Vol. 147 (2), pp. 323–331.
- [23] Dudley, P., Bonazza, R., Porter, and W.P., 2016, "Climate change impacts on nesting and internesting leatherback sea turtles using 3D animated computational fluid dynamics and finite volume heat transfer", *Ecological Modelling*, Vol. 320, pp. 231–240.
- [24] Paladino, F., O'Connor, M., and Spotila, J., 1990, "Metabolism of leatherback turtles, gigantothermy, and thermoregulation of dinosaurs", *Nature*, Vol. 344 (6269), pp. 858–860.
- [25] Versteeg, H., and Malalasekera, W., 2007, An introduction to computational fluid dynamics: the finite volume method, Pearson Education Limited, second edn.
- [26] Menter, F., and Esch, T., 2001, "Elements of Industrial Heat Transfer Predictions", Vol. 20, pp. 117–127.
- [27] Menter, F. R., Kuntz, M., and Langtry, R., 2003, "Ten Years of Industrial Experience with the SST Turbulence Model", *Heat and Mass Transfer*, Begell House, pp. 625–632.
- [28] Motani, R., 2002, "Swimming speed estimation of extinct marine reptiles: energetic approach revisited", *Paleobiology*, Vol. 28 (2), pp. 251–262
- [29] Schwartz, F., 1978, "Behavioral and tolerance responses to cold water temperatures by three species of sea turtles (Reptilia, Cheloniidae) in North Carolina", *Florida Marine Research Publications*, (33), pp. 16–18.
- [30] Kubo, T., Mitchell, M. T., and Henderson, D. M., 2012, "Albertonectes vanderveldei, a new elasmosaur (Reptilia, Sauropterygia) from the Upper Cretaceous of Alberta", *Journal of Vertebrate Paleontology*, Vol. 32 (3), pp. 557– 572.